KU LEUVEN

STADIUS
Center for Dynamical Systems, Signal Processing and Data Analytics

Citation/Reference	Bernardi G., van Waterschoot T., Wouters J., and Moonen M. (2015), **An All-Frequency-Domain Adaptive Filter with PEM-Based Decorrelation for Acoustic Feedback Control** Proc. 2015 IEEE Workshop on Applications of Signal Process. to Audio and Acoustics (WASPAA 15), New Paltz, NY, Oct. 2015, pp. 1--5.
Archived version	Author manuscript: the content is identical to the content of the published paper, but without the final typesetting by the publisher
Published version	http://ieeexplore.ieee.org/xpl/articleDetails.jsp?arnumber=7336931
Journal homepage	http://www.waspaa.com/
Author contact	giuliano.bernardi@esat.kuleuven.be *+ 32 (0)16 321797*
IR	

(article begins on next page)

AN ALL-FREQUENCY-DOMAIN ADAPTIVE FILTER WITH PEM-BASED DECORRELATION FOR ACOUSTIC FEEDBACK CONTROL

Giuliano Bernardi[†], *Toon van Waterschoot*[†*], *Jan Wouters*[§] *and Marc Moonen*[†]

[†]KU Leuven, Dept. of Electrical Engineering (ESAT-STADIUS), Kasteelpark Arenberg 10, 3001 Leuven, Belgium

[*]KU Leuven, Dept. of Electrical Engineering (ESAT-ETC), AdvISe Lab, Kleinhoefstraat, 2440 Geel, Belgium

[§]KU Leuven, Dept. of Neurosciences (ExpORL), Herestraat 49 bus 721, 3000 Leuven, Belgium

ABSTRACT

A new method for acoustic feedback control is derived, combining an adaptive filter with a decorrelation strategy based on the prediction-error method (PEM) entirely in the frequency domain. This all-frequency-domain method extends existing methods combining a frequency-domain adaptive filter (FDAF) and time-domain PEM-based decorrelation. Such a combined approach is critical, since a standard adaptive feedback cancellation (AFC) procedure without proper decorrelation yields biased estimation results and hence does not provide suitable acoustic feedback control. The proposed modification allows to lower the computational complexity of the algorithm, while maintaining comparable performance.

Index Terms— Adaptive feedback cancellation (AFC), prediction-error method (PEM), frequency-domain adaptive filter (FDAF), acoustic feedback control

1. INTRODUCTION

Frequency-domain adaptive filter (FDAF) implementations have been extensively used in digital signal processing, since their introduction more than two decades ago, given the advantages they offer compared to classical time-domain implementations. Not only can a frequency-domain implementation lead to a reduction in the computational complexity of the algorithm, working in the frequency-domain also allows to exploit the decorrelation properties of the discrete Fourier transform to achieve improved performance [1, 2, 3].

Several applications employing a FDAF implementation require additional operations to provide the assumed working conditions for the adaptive filter. An example of such additional operations is a decorrelation, necessary to reduce the correlation between the adaptive filter desired signal and undesired interference, inherent in a closed-loop system identification scenario. A whitening prefilter based on the prediction-error method (PEM) can be successfully applied for decorrelation [4].

Acoustic feedback control is an application example commonly addressed using adaptive feedback cancellation (AFC), which indeed requires an additional decorrelation. This can be understood referring to Fig. 1, by noticing that the desired signal $v(t)$ and the undesired interference $x(t)$ are related by a closed-loop transfer function (TF) [5]. The closed-loop TF depends on the different TFs characterizing the system, depicted as blocks in Fig. 1: $F(q,t)$ and $\hat{F}(q,t)$ represent the true and estimated feedback path, respectively, and $G(q,t)$ represents the forward path. All the TFs are defined by means of the delay operator q^{-1}, i. e. $q^{-k}u(t) = u(t-k)$.

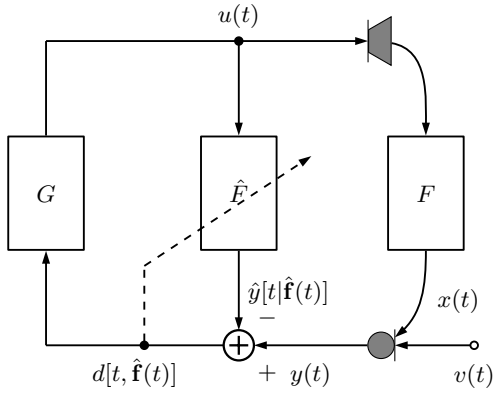

Figure 1: General AFC scenario.

The use of a standard adaptive filter in this scenario leads to a biased estimate $\hat{F}(q,t)$, due to the correlation between $v(t)$ and $x(t)$ [6]. The problem of a biased estimate is exacerbated by the presence of the closed-loop system, in which a poor estimation can also induce unstable behavior such as howling. Therefore, a procedure to effectively decorrelate $v(t)$ and $x(t)$ must be introduced.

Different methods combining the use of an adaptive filter and a PEM-based prefilter for the decorrelation have been discussed in several papers: the earliest such method relies on time-domain implementations for both the adaptive filter and the PEM-based decorrelation [6, 7, 8]. A time-domain implementation for the decorrelation combined with a FDAF, referred to as PEM-based frequency-domain adaptive filter (PEM-FDAF), has also been proposed [2, 9].

In this paper, we present a modification of the existing methods providing a frequency-domain implementation of both the adaptive filter and the PEM-based decorrelation. This all-frequency-domain method reduces the computational complexity of the PEM-FDAF while maintaining comparable performance. Moreover, by means of some simplifications, the new method allows to lump all the decorrelation operations into the adaptive filter stepsize, possibly leading to a new interesting interpretation of the decorrelation role.

In Section 2, we introduce the existing PEM-FDAF method with time-domain PEM-based decorrelation. In Section 3, we derive the all-frequency-domain method relying on frequency-domain PEM-based decorrelation and, in Section 4, we provide a computa-

This research work was carried out at the ESAT Laboratory and at the ExpORL Laboratory of KU Leuven, in the frame of the IWT O&O Project nr. 110722 'Signal processing and automatic fitting for next generation cochlear implants', KU Leuven Research Council CoE PFV/10/002 (OPTEC), the Interuniversity Attractive Poles Programme initiated by the Belgian Science Policy Office: IUAP P7/19 'Dynamical systems control and optimization' (DYSCO) 2012-2017. The scientific responsibility is assumed by its authors.

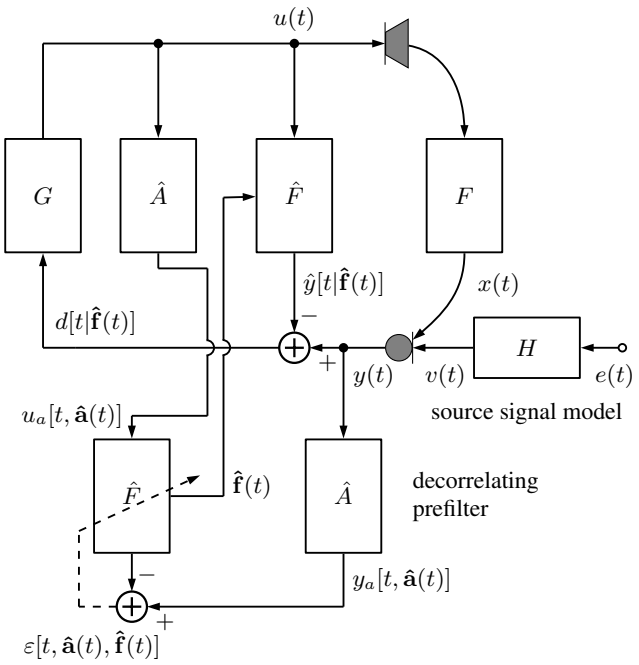

Figure 2: Block diagram of an AFC including PEM-based decorrelation.

tional complexity comparison. In Section 5, we show some simulation results highlighting the similarity between existing and proposed methods, in terms of convergence, added stability and sound quality. Finally, the conclusions are drawn in Section 6.

2. PEM-BASED FREQUENCY-DOMAIN ADAPTIVE FILTER (PEM-FDAF)

The PEM-FDAF method [2, 9] for AFC can be derived from the standard FDAF, by introducing a set of prefiltering operations, as illustrated in Fig. 2. The microphone signal $y(t)$ represents the sum of the desired source signal $v(t)$ and the undesired feedback signal $x(t)$. The true acoustic feedback path $\mathbf{f}(t)$ is assumed to be of known, finite order n_F and is estimated by the adaptive filter $\hat{\mathbf{f}}(t)$, of order $n_{\hat{F}} = n_F$; the estimate $\hat{\mathbf{f}}(t)$ is then used to calculate $\hat{y}[t|\hat{\mathbf{f}}(t)]$, i. e. a prediction of the undesired signal $x(t)$, in order to remove the contribution of $x(t)$ from the microphone signal $y(t)$.

The additional blocks in Fig. 2, compared to Fig. 1, define the time-varying autoregressive (AR) source signal model $H(q,t) = \frac{1}{A(q,t)}$ and the estimated inverse source signal model $\hat{A}(q,t)$, both of order n_H. By means of $H(q,t)$, the source signal $v(t)$ can be modeled using the white noise sequence $e(t)$ as input signal, i. e. $v(t) = H(q,t)e(t)$. The modeling choice on $H(q,t)$ is done since a low-order AR model has been shown to provide a good approximation for speech signals [10, 11]. The role of $\hat{A}(q,t)$ is to prefilter the microphone, loudspeaker and hence the error signal, obtaining $y_a[t, \hat{\mathbf{a}}(t)]$, $u_a[t, \hat{\mathbf{a}}(t)]$ and $\varepsilon[t, \hat{\mathbf{a}}(t), \hat{\mathbf{f}}(t)]$, respectively, used to perform the adaptation procedure. In the following, the dependencies on $\hat{\mathbf{a}}(t)$ and $\hat{\mathbf{f}}(t)$ will be omitted.

To describe the PEM-FDAF algorithm, we must first introduce the discrete time frame and frequency frame variables, k and l, respectively. The M-samples loudspeaker signal frame at (frame) time $k \in \mathbb{Z}$ and its prefiltered version are defined as follows:

$$\mathbf{u}(k) = [u(kL - M + 1) \quad \dots \quad u(kL)]^{\mathrm{T}} \tag{1a}$$

$$\mathbf{u}_a(k) = [u_a(kL - M + 1) \quad \dots \quad u_a(kL)]^{\mathrm{T}}, \tag{1b}$$

with L denoting the frame shift.

The microphone signal frame and its prefiltered version are constrained to R-samples — typically $R = L = M/2$ and $R = n_{\hat{F}}$ [1, 9] — to accommodate for the overlap-and-save procedure:

$$\mathbf{y}(k) = [y(kL - R + 1) \quad \dots \quad y(kL)]^{\mathrm{T}} \tag{2a}$$

$$\mathbf{y}_a(k) = [y_a(kL - R + 1) \quad \dots \quad y_a(kL)]^{\mathrm{T}}. \tag{2b}$$

For the loudspeaker and microphone signal, the prefiltering can be expressed as follows:

$$u_a(kL - j) = \hat{A}(q,k)u(kL - j) \quad j = 0, \dots, M-1 \tag{3a}$$

$$y_a(kL - j) = \hat{A}(q,k)y(kL - j) \quad j = 0, \dots, R-1. \tag{3b}$$

The frequency-domain versions of the loudspeaker signal frame, before and after prefiltering, can be expressed introducing the discrete Fourier transform matrix $\mathbf{F}_M$ of size $M \times M$:

$$\mathbf{U}(k) = \mathrm{diag}\left\{\mathbf{F}_M \mathbf{u}(k)\right\} \tag{4a}$$

$$\mathbf{U}_a(k) = \mathrm{diag}\left\{\mathbf{F}_M \mathbf{u}_a(k)\right\}. \tag{4b}$$

The error signal frame is defined as the difference between the microphone signal frame and the estimated feedback signal frame, where the latter is calculated in the frequency domain by circular convolution, linearized via the projection matrix $\mathbf{Q} = [\mathbf{0}_R \quad \mathbf{I}_R]^{\mathrm{T}}$:

$$\mathbf{d}(k) = \mathbf{y}(k) - \hat{\mathbf{y}}(k) \tag{5a}$$

$$\hat{\mathbf{y}}(k) = \mathbf{Q}^{\mathrm{T}}\mathbf{F}_M^{-1}\mathbf{U}(k)\hat{\mathbf{F}}(k), \tag{5b}$$

with $\hat{\mathbf{F}}(k) = \mathbf{F}_M \begin{bmatrix}\hat{\mathbf{f}}^{\mathrm{T}}(k) & \mathbf{0}_{1\times R}\end{bmatrix}^{\mathrm{T}}$.

The AR coefficients $\hat{\mathbf{a}}(k) = [1 \quad \hat{a}_1(k) \quad \dots \quad \hat{a}_{n_H}(k)]^{\mathrm{T}}$ estimate the denominator coefficients of $H(q,k)$ and, equivalently, define the numerator coefficients of $\hat{A}(q,k)$. These coefficients are estimated using the Levinson-Durbin algorithm [12, pp. 254-264] on the concatenation of the error signal frames $\mathbf{d}(k)$ and $\mathbf{d}(k-1)$, and are used to calculate the prefiltered quantities $\mathbf{u}_a(k)$ and $\mathbf{y}_a(k)$, cf. (3), (1b) and (2b). The prediction error signal frame $\boldsymbol{\varepsilon}(k)$ is, in turn, obtained by means of these prefiltered quantities:

$$\boldsymbol{\varepsilon}(k) = \mathbf{y}_a(k) - \hat{\mathbf{y}}_a(k) \tag{6a}$$

$$\hat{\mathbf{y}}_a(k) = \mathbf{Q}^{\mathrm{T}}\mathbf{F}_M^{-1}\mathbf{U}_a(k)\hat{\mathbf{F}}(k). \tag{6b}$$

Finally, the prediction error signal frame is transformed to the frequency domain and used, together with the frequency-domain prefiltered loudspeaker signal frame, in the stochastic gradient iteration to update the estimated $\hat{\mathbf{F}}(k)$:

$$\boldsymbol{\mathcal{E}}(k) = \mathbf{F}_M \mathbf{Q}\boldsymbol{\varepsilon}(k) \tag{7a}$$

$$\Delta\hat{\mathbf{F}}(k) = \mathrm{diag}\{\boldsymbol{\mu}(k)\}\mathbf{U}_a^{\mathrm{H}}(k)\boldsymbol{\mathcal{E}}(k) \tag{7b}$$

$$\hat{\mathbf{F}}(k+1) = \hat{\mathbf{F}}(k) + \mathbf{F}_M\left[\mathbf{I}_M - \mathbf{Q}\mathbf{Q}^{\mathrm{T}}\right]\mathbf{F}_M^{-1}\Delta\hat{\mathbf{F}}(k). \tag{7c}$$

The stepsize $\boldsymbol{\mu}(k)$ normalizes $\Delta\hat{\mathbf{F}}(k)$ using the instantaneous power of the adaptive procedure's reference signal, and its l-th element at time k is defined as follows:

$$\mu(k,l) = \mu_{\mathrm{fix}}\left[\alpha + |U_a(k,l)|^2\right]^{-1}, \tag{8}$$

where μ_{fix} is a real, constant, and frequency-independent value. A summary of the PEM-FDAF algorithm is given in Algorithm 1.

Algorithm 1 PEM-based Frequency-domain adaptive filter (PEM-FDAF) [9].

Initialize $R = L = M/2$, $\hat{\mathbf{F}}(0) = \mathbf{d}(0) = \mathbf{0}_{M\times 1}$
for $k = 1, 2, \ldots$ **do**
  $\mathbf{U}(k) = \text{diag}\left\{\mathbf{F}_M \left[u(kL - M + 1), \ldots, u(kL)\right]^{\text{T}}\right\}$
  $\hat{\mathbf{y}}(k) = \mathbf{Q}^{\text{T}}\mathbf{F}_M^{-1}\mathbf{U}(k)\hat{\mathbf{F}}(k)$
  $\mathbf{d}(k) = \mathbf{y}(k) - \hat{\mathbf{y}}(k)$
  $\hat{\mathbf{a}}(k) = \texttt{Levinson} - \texttt{Durbin}\left([\mathbf{d}(k); \mathbf{d}(k-1)]\right)$
  $u_a(kL - j) = \hat{A}(q, k)u(kL - j), \quad j = 0, \ldots, M - 1$
  $y_a(kL - j) = \hat{A}(q, k)y(kL - j), \quad j = 0, \ldots, R - 1$
  $\mathbf{U}_a(k) = \text{diag}\left\{\mathbf{F}_M \mathbf{u}_a(k)\right\}$
  $\hat{\mathbf{y}}_a(k) = \mathbf{Q}^{\text{T}}\mathbf{F}_M^{-1}\mathbf{U}_a(k)\hat{\mathbf{F}}(k)$
  $\boldsymbol{\varepsilon}(k) = \mathbf{y}_a(k) - \hat{\mathbf{y}}_a(k)$
  $\boldsymbol{\mathcal{E}}(k) = \mathbf{F}_M\mathbf{Q}\boldsymbol{\varepsilon}(k)$
  $\mu(k, l) = \mu_{\text{fix}}\left[\alpha + |U_a(k, l)|^2\right]^{-1}$
  $\Delta\hat{\mathbf{F}}(k) = \text{diag}\{\boldsymbol{\mu}(k)\}\mathbf{U}_a^{\text{H}}(k)\boldsymbol{\mathcal{E}}(k)$
  $\hat{\mathbf{F}}(k + 1) = \hat{\mathbf{F}}(k) + \mathbf{F}_M\left[\mathbf{I}_M - \mathbf{Q}\mathbf{Q}^{\text{T}}\right]\mathbf{F}_M^{-1}\Delta\hat{\mathbf{F}}(k)$
end for

3. FREQUENCY-DOMAIN PEM-BASED ADAPTIVE FILTER (FD-PEMAF)

The proposed all-frequency-domain method, referred to as frequency-domain PEM-based adaptive filter (FD-PEMAF), modifies the PEM-FDAF by performing the prefiltering operations in the frequency-domain. The prefilter is still estimated from the time-domain error signal, but the adaptive filter calculation is now fully in the frequency domain. In order to implement the prefiltering operations correctly, the frame shift is reduced by a number of samples equal to the prefilter length, i. e. from R to $L = R - n_H$. The vector of AR coefficients $\hat{\mathbf{a}}(k)$ is estimated as in the PEM-FDAF, and subsequently transformed to the frequency domain:

$$\hat{\mathbf{A}}(k) = \text{diag}\left\{\mathbf{F}_M\left[\hat{\mathbf{a}}^{\text{T}}(k) \quad \mathbf{0}_{1\times(M-n_H-1)}\right]^{\text{T}}\right\}. \tag{9}$$

The L-samples prediction error signal frame $\boldsymbol{\varepsilon}(k)$ is defined by means of (9), and transformed to the frequency domain as follows:

$$\boldsymbol{\varepsilon}(k) = \mathbf{Q}_{n_H}^{\text{T}}\mathbf{F}_M^{-1}\hat{\mathbf{A}}(k)[\mathbf{Y}(k) - \mathbf{U}(k)\hat{\mathbf{F}}(k)] \tag{10a}$$
$$\boldsymbol{\mathcal{E}}(k) = \mathbf{F}_M\mathbf{Q}_{n_H}\boldsymbol{\varepsilon}(k). \tag{10b}$$

Equation (10a) includes the frequency-domain version of the microphone signal frame $\mathbf{Y}(k) = \mathbf{F}_M\mathbf{Q}\mathbf{y}(k)$, and provides the concurrent frequency-domain filtering of the microphone signal frame $\mathbf{y}(k)$, via the prefilter $\hat{\mathbf{a}}(k)$, and of the loudspeaker signal frame $\mathbf{u}(k)$, via the prefilter $\hat{\mathbf{a}}(k)$ and the feedback path $\hat{\mathbf{f}}(k)$. As the prediction error signal frame $\boldsymbol{\varepsilon}(k)$ is n_H-samples shorter than the error signal $\mathbf{d}(k)$, $\mathbf{Q} \neq \mathbf{Q}_{n_H} = \begin{pmatrix}\mathbf{0}_{L\times R+n_H} & \mathbf{I}_L\end{pmatrix}^{\text{T}}$.

The definition of $\Delta\hat{\mathbf{F}}(k)$, cf. (7b), will then become:

$$\Delta\hat{\mathbf{F}}(k) = \text{diag}\{\boldsymbol{\mu}(k)\}\hat{\mathbf{A}}^{\text{H}}(k)\mathbf{U}^{\text{H}}(k)\boldsymbol{\mathcal{E}}(k). \tag{11}$$

This new definition does not require the explicit calculation of the frequency-domain prefiltered loudspeaker signal $\mathbf{U}_a(k)$, thus leading to a slightly modified definition of the adaptive stepsize $\mu(k, l)$, cf. Algorithm 1 and 2.

A different definition of $\Delta\hat{\mathbf{F}}(k)$ can be obtained by approximating the linearization constraint $\mathbf{G}_{n_H} = \mathbf{F}_M\mathbf{Q}_{n_H}\mathbf{Q}_{n_H}^{\text{T}}\mathbf{F}_M^{-1}$ as

Algorithm 2 Constrained and unconstrained frequency-domain PEM-based adaptive filter (FD-PEMAF and uFD-PEMAF, respectively).

Initialize $M = 2R$, $L = R - n_H$, $\hat{\mathbf{F}}(0) = \mathbf{d}(0) = \mathbf{0}_{M\times 1}$
for $k = 1, 2, \ldots$ **do**
  $\mathbf{U}(k) = \text{diag}\left\{\mathbf{F}_M \left[u(kL - M + 1), \ldots, u(kL)\right]^{\text{T}}\right\}$
  $\mathbf{Y}(k) = \mathbf{F}_M\mathbf{Q}\mathbf{y}(k)$
  $\mathbf{d}(k) = \mathbf{y}(k) - \mathbf{Q}^{\text{T}}\mathbf{F}_M^{-1}\mathbf{U}(k)\hat{\mathbf{F}}(k)$
  $\hat{\mathbf{a}}(k) = \texttt{Levinson} - \texttt{Durbin}\left([\mathbf{d}(k); \mathbf{d}(k-1)]\right)$
  $\hat{\mathbf{A}}(k) = \text{diag}\left\{\mathbf{F}_M\left[\hat{\mathbf{a}}^{\text{T}}(k) \quad \mathbf{0}_{1\times(M-n_H-1)}\right]^{\text{T}}\right\}$
  if unconstrained **then**
    $\mathbf{G}_{n_H} \approx L/M \cdot \mathbf{I}_M$
  else
    $\mathbf{G}_{n_H} = \mathbf{F}_M\mathbf{Q}_{n_H}\mathbf{Q}_{n_H}^{\text{T}}\mathbf{F}_M^{-1}$
  end if
  $\boldsymbol{\mathcal{E}}(k) = \mathbf{G}_{n_H}\hat{\mathbf{A}}(k)[\mathbf{Y}(k) - \mathbf{U}(k)\hat{\mathbf{F}}(k)]$
  $\mu(k, l) = \mu_{\text{fix}}\left[\alpha + |U(k, l)\hat{A}(k, l)|^2\right]^{-1}$
  $\Delta\hat{\mathbf{F}}(k) = \text{diag}\{\boldsymbol{\mu}(k)\}\hat{\mathbf{A}}^{\text{H}}(k)\mathbf{U}^{\text{H}}(k)\boldsymbol{\mathcal{E}}(k)$
  $\hat{\mathbf{F}}(k + 1) = \hat{\mathbf{F}}(k) + \mathbf{F}_M\left[\mathbf{I}_M - \mathbf{Q}\mathbf{Q}^{\text{T}}\right]\mathbf{F}_M^{-1}\Delta\hat{\mathbf{F}}(k)$
end for

$\mathbf{G}_{n_H} \approx L/M \cdot \mathbf{I}_M$ in the calculation of $\boldsymbol{\mathcal{E}}(k)$, as suggested by Benesty et al. [13, pp. 168-170], leading to

$$\Delta\hat{\mathbf{F}}(k) = L/M \cdot \text{diag}\{\boldsymbol{\mu}(k)\}\hat{\mathbf{A}}(k)\hat{\mathbf{A}}^{\text{H}}(k)\mathbf{U}^{\text{H}}(k)\mathbf{D}(k), \tag{12}$$

where the order of the multiplications has been changed, due to the diagonality of both $\hat{\mathbf{A}}(k)$ and $\mathbf{U}(k)$. Equations (11) and (12) are not equivalent, and the substitution of (11) with (12) results in a modified algorithm referred to as unconstrained FD-PEMAF (uFD-PEMAF). The motivation to choose an unconstrained version could arise, for instance, if complexity is an issue [1], since dropping the constraints allows to save two FFT operations per iteration.

Equation (12) allows to lump all the prefiltering operations into the stepsize, obtaining:

$$\text{diag}\{\boldsymbol{\mu}_a(k)\} = L/M \cdot \text{diag}\{\boldsymbol{\mu}(k)\}\hat{\mathbf{A}}(k)\hat{\mathbf{A}}^{\text{H}}(k) \tag{13a}$$
$$\Delta\hat{\mathbf{F}}(k) = \text{diag}\{\boldsymbol{\mu}_a(k)\}\mathbf{U}^{\text{H}}(k)\mathbf{D}(k). \tag{13b}$$

A summary of the FD-PEMAF is given in Algorithm 2.

In Section 1, we mentioned that prefiltering is introduced to reduce the bias of the feedback path estimate by providing some degree of decorrelation between the loudspeaker and microphone signal. Therefore, lumping the prefilter contribution into the stepsize extends the usual set of measures affected by stepsize tuning, namely convergence speed, stability and steady-state error [12], by the estimation bias. Such a representation thus provides an interesting insight into the role of the stepsize. However, unlike other unconstrained FDAF algorithms [1], our results will show a strong performance decrease, making it a rather unappealing choice.

4. COMPUTATIONAL COMPLEXITY

In this section, we provide a complexity comparison between existing and proposed algorithms, focusing on the number of per-sample real multiplications. Assuming equal complexity for a real multiplication and a real division, a complexity of $M \log_2(M)$ for each FFT/IFFT operation [1], a real, frequency-dependent stepsize, and a

Table 1: Per-sample computational complexity of the algorithms.

Algorithm	Real multiplications
PEM-FDAF	$\frac{7M\log_2(M)+19M+R+3n_H^2+n_H(7+2M+R)}{R-n_H}$
FD-PEMAF	$\frac{8M\log_2(M)+22M+n_H^2+n_H(5+M)}{R-n_H}$
uFD-PEMAF	$\frac{6M\log_2(M)+22M+n_H^2+n_H(5+M)}{R-n_H}$

total cost of $n_H^2+(5+M)n_H+M$ for the Levinsion-Durbin calculations [12], the three algorithms have the computational complexities shown in Table 1. The FD-PEMAF requires one additional FFT operation compared to the PEM-FDAF, as seen in the first factor at numerator in the complexity calculations, but limits the overall complexity by removing the time-domain prefiltering operations.

Using the values chosen in the simulations discussed in the following section, i. e. $M = 160$, $R = 80$, $n_H = 15$ and $L = 65$, the cost for each new processed sample is 278, 240 and 204 for PEM-FDAF, FD-PEMAF and uFD-PEMAF, respectively. This corresponds to a complexity decrease of 14 % for FD-PEMAF and 27 % for uFD-PEMAF, when compared with PEM-FDAF.

5. SIMULATION RESULTS

The performance of the algorithms is assessed by means of three standard measures evaluating the estimation error, the achievable amplification and the sound quality. The estimation error is evaluated using the misadjustment (Mis), i. e. the normalized distance between the true and estimated feedback path [5]; the achievable amplification is assessed via the added stable gain (ASG), i. e. the increase of the maximum stable gain (MSG) due to the inclusion of the adaptive filter, assuming a spectrally flat $G(q,t)$ [2]; the sound quality is evaluated using the so-called frequency-weighted log-spectral signal distortion (SD), providing good correlation with subjective evaluations in feedback cancellation tasks [14].

Clean speech, sampled at $f_s = 16$ kHz was chosen as the source signal $v(k)$, while the feedback path $F(q,t)$ was measured in a commercial hearing aid [2]. The TF $G(q,t)$ was characterized by a delay of 65 samples and two broadband gain values: the first, referred to as K_1, corresponded to 3 dB below the MSG obtained without the inclusion of $\hat{F}(q,t)$; the second, referred to as K_2, was set to $K_2 = K_1 + 10$ dB. The estimated AR model for $v(t)$ was fixed to 15, similar to the usual low-order values used in literature [11, 15], and the frame parameters were chosen to be $M = 160$, $R = 80$ and $L = 65$ (for the PEM-FDAF too), as previously mentioned. Finally, the fixed step size and the regularization constant were set to $\mu_{\text{fix}} = 0.01$ and $\alpha = 5 \times 10^{-5}$, respectively.

The first set of results for Mis and ASG refers to the K_1 condition and is shown using dotted lines in Fig. 3. After 10 s, both PEM-FDAF and FD-PEMAF reach some -8 dB of Mis, roughly 6 dB lower than uFD-PEMAF; similar results, with the opposite sign, exists for the ASG results (8 dB for PEM-FDAF and FD-PEMAF, and 2 dB uFD-PEMAF) after 8 s, but the constrained versions undergo a performance deterioration toward the end of the simulation, possibly due to the specific signal characteristics in such time interval. The performance mismatch between PEM-FDAF and FD-PEMAF can be attributed to the different calculation of $\mu(k,l)$, cf. Algorithm 1 and 2.

The second set of results for Mis and ASG refers to the K_2 condition and is shown using solid lines in Fig. 3. In this case, the Mis

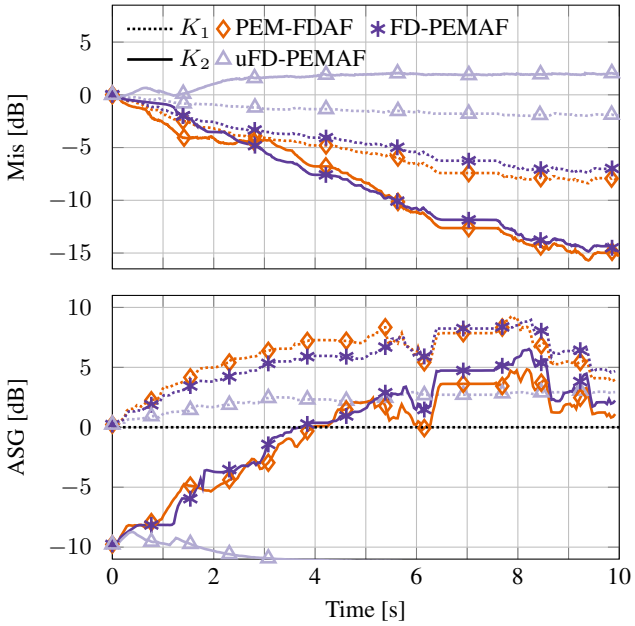

Figure 3: Mis and ASG performance for the three algorithms using the two tested gains.

Table 2: Mean and maximum SD values for the different algorithms in the two tested scenarios.

	mean(SD)		max(SD)	
	K_1	K_2	K_1	K_2
PEM-FDAF	1.52	1.83	4.16	4.38
FD-PEMAF	1.74	2.25	4.21	4.49
uFD-PEMAF	2.79	41.96	5.23	67.53

values after 10 s for PEM-FDAF and FD-PEMAF are both shifted by roughly -7 dB, while uFD-PEMAF has now convergence problems. The ASG results after 10 s for PEM-FDAF and FD-PEMAF are approximately 3 dB lower than in the K_1 condition, but both algorithms need almost 4 s to reach a greater-than-zero ASG. On the contrary, uFD-PEMAF remains heavily unstable (ASG < -8 dB) throughout the whole simulation.

Table 2 lists the sound quality results, by means of mean and maximum SD. Similar results, in both tested conditions, are obtained for PEM-FDAF and FD-PEMAF, while uFD-PEMAF shows a worse performance, severely worsened in the K_2 condition.

The simulation results presented in this section suggest that comparable performance is expected with PEM-FDAF and FD-PEMAF, whereas a stronger degradation can be expected using uFD-PEMAF, making the latter a highly discouraged choice.

6. CONCLUSIONS

An all-frequency-domain method for AFC has been derived, allowing to reduce the computational complexity of the PEM-FDAF while maintaining comparable performance in terms of estimation error, achievable amplification and sound-quality performance.

An additional simplification obtained by dropping a linearization constraint and allowing to interpret the stepsize multiplication of the adaptive algorithm as a decorrelation operation, has been shown to dramatically worsen the reference performance, especially for higher values of the forward path gain. Therefore, such a simplification is highly discouraged.

7. REFERENCES

[1] J. J. Shynk, "Frequency-domain and multirate adaptive filtering," *Signal Processing Magazine, IEEE*, vol. 9, no. 1, pp. 14 –37, Jan 1992.

[2] A. Spriet, G. Rombouts, M. Moonen, and J. Wouters, "Adaptive feedback cancellation in hearing aids," *Journal of the Franklin Institute*, vol. 343, no. 6, pp. 545 – 573, Aug 2006.

[3] J. M. Gil-Cacho, T. van Waterschoot, M. Moonen, and S. Jensen, "Transform domain prediction error method for improved acoustic echo and feedback cancellation," in *Proc. 20th Eur. Signal Process. Conf. (EUSIPCO)*, Bucharest, Romania, Aug 2012, pp. 2422–2426.

[4] U. Forssell and L. Ljung, "Closed-loop identification revisited," *Automatica*, vol. 35, no. 7, pp. 1215 – 1241, Jul 1999.

[5] T. van Waterschoot and M. Moonen, "Fifty years of acoustic feedback control: State of the art and future challenges," *Proceedings of the IEEE*, vol. 99, no. 2, pp. 288 –327, Feb 2011.

[6] J. Hellgren and U. Forssell, "Bias of feedback cancellation algorithms in hearing aids based on direct closed loop identification," *Speech and Audio Processing, IEEE Transactions on*, vol. 9, no. 8, pp. 906 –913, Nov 2001.

[7] G. Rombouts, T. van Waterschoot, K. Struyve, and M. Moonen, "Acoustic feedback cancellation for long acoustic paths using a nonstationary source model," *IEEE Transactions on Signal Processing*, vol. 54, no. 9, pp. 3426–3434, Sep 2006.

[8] A. Spriet, I. Proudler, M. Moonen, and J. Wouters, "Adaptive feedback cancellation in hearing aids with linear prediction of the desired signal," *Signal Processing, IEEE Transactions on*, vol. 53, no. 10, pp. 3749–3763, Oct 2005.

[9] J. M. Gil-Cacho, T. van Waterschoot, M. Moonen, and S. H. Jensen, "A frequency-domain adaptive filter (FDAF) prediction error method (PEM) framework for double-talk-robust acoustic echo cancellation," *Audio, Speech, and Language Processing, IEEE/ACM Transactions on*, vol. 22, no. 12, pp. 2074–2086, Dec 2014.

[10] J. Makhoul, "Linear prediction: A tutorial review," *Proceedings of the IEEE*, vol. 63, no. 4, pp. 561 – 580, Apr 1975.

[11] T. van Waterschoot, G. Rombouts, P. Verhoeve, and M. Moonen, "Double-talk-robust prediction error identification algorithms for acoustic echo cancellation," *Signal Processing, IEEE Transactions on*, vol. 55, no. 3, pp. 846 –858, Mar 2007.

[12] S. Haykin, *Adaptive filter theory*, ser. Prentice-Hall information and system sciences series. Prentice Hall, 2002.

[13] J. Benesty, T. Gänsler, D. R. Morgan, M. M. Sondhi, and S. L. Gay, *Advances in Network and Acoustic Echo Cancellation*, ser. Digital Signal Processing. Springer, 2001.

[14] A. Spriet, K. Eneman, M. Moonen, and J. Wouters, "Objective measures for real-time evaluation of adaptive feedback cancellation algorithms in hearing aids," in *Proc. 16th Eur. Signal Process. Conf. (EUSIPCO)*, Lausanne, Switzerland, Aug 2008.

[15] T. van Waterschoot, G. Rombouts, and M. Moonen, "Optimally regularized adaptive filtering algorithms for room acoustic signal enhancement," *Signal Processing*, vol. 88, no. 3, pp. 594 – 611, Mar 2008.